Monatshefte für Chemie 136, 489–508 (2005)
DOI 10.1007/s00706-004-0278-3

Monatshefte für Chemie
Chemical Monthly
Printed in Austria

Exciton Chirality. (A) Origins of and (B) Applications from Strongly Fluorescent Dipyrrinone Chromophores

Stefan E. Boiadjiev and **David A. Lightner***

Department of Chemistry, University of Nevada, Reno, Nevada 89557, USA

Received October 5, 2004; accepted (revised) November 10, 2004
Published online March 8, 2005 © Springer-Verlag 2005

Summary. (A) The origin of exciton interaction and examples of its application to organic stereochemistry are presented. (B) *N*,*N*′-Carbonyl-bridged dipyrrinones constitute a new class of highly fluorescent chromophores suitable for investigations of stereochemistry and absolute configuration. *N*,*N*′-Carbonylxanthobilirubic acid esters are strongly fluorescent, with a fluorescence quantum yield (ϕ_F) ~0.8, but produce only weak exciton CD from the *trans*-1,2-cyclohexanediol template. The ester of an analog with benzoic acid replacing propionic, *N*,*N*′-carbonyl-8-(4-carboxyphenyl)-3-ethyl-2,7,9-trimethyl-(10*H*)-dipyrrin-1-one, exhibits strong fluorescence ($\phi_F = 0.68$, $\lambda_{em} = 493$ nm, $\lambda_{ex} = 422$ nm in $CHCl_3$) and UV-Vis absorption ($\varepsilon \sim 21000$ at 424 nm) in organic solvents. Its diester with (1*S*,2*S*)-cyclohexanediol is fluorescent and exhibits exciton circular dichroism ($\Delta\varepsilon = +15\,dm^3 \cdot mol^{-1} \cdot cm^{-1}$, $\lambda = 432$ nm; $\Delta\varepsilon = -4\,dm^3 \cdot mol^{-1}\,cm^{-1}$, $\lambda = 380$ nm) that correlates with the *Exciton Chirality Rule*.

Keywords. Circular Dichroism; Fluorescence; Exciton; Pyrroles.

Part A. Fundamentals of Exciton Chirality

Exciton Coupling

Exciton Spectra. Excitation of a molecule from its electronic *ground state* to an electronically *excited state* – promoted usually by the absorption of ultraviolet or visible light – involves movement of an electron, a process called an electronic transition. In near ultraviolet-visible light absorption, the electron typically moves from a high-energy occupied molecular orbital to a low-energy unoccupied molecular orbital, such as in $\pi \rightarrow \pi^*$ excitations. This movement of an electron creates an instantaneous dipole or polarization of charge (called an electric transition moment or electric transition dipole), a vector quantity with both a direction (orientation) and a magnitude (intensity) that vary according to the nature of the particular electronic transition and the chromophore involved. Two or more

* Corresponding author. E-mail: lightner@scs.unr.edu

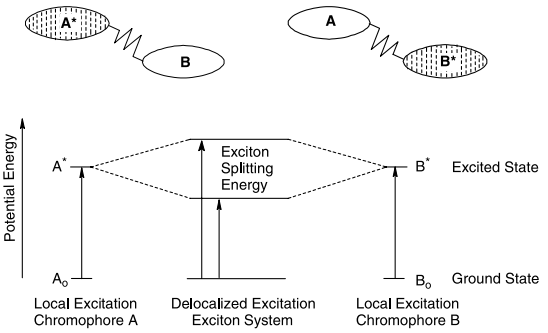

Fig. 1. Diagrammatic representation of exciton coupling between two chromophores (A and B) fastened together by covalent bonding or intermolecular forces; local excitations are shown (left and right) for the chromophores in their locally excited monomer states (A^* or B^*); when the two chromophores lie sufficiently close to one another, or the local excitations are sufficiently intense, excitation is delocalized between the two chromophores and the excited state (exciton) is split by resonance interaction of the local excitations in the composite system or molecule (center); exciton coupling may take place between identical chromophores ($A = B$) or non-identical chromophores ($A \neq B$) and is less effective when the excitation energies are very different, *i.e.*, when the relevant UV-Vis absorption bands do not overlap

chromophores, brought into proximity to one another, may interact with each other (even when orbital overlap and electron exchange are negligible) when one chromophore is excited electronically. That is, when the electronic transitions associated with two chromophores have similar energies (*e.g.*, λ) and intensities (*e.g.*, ε), the electric transition dipole of one chromophore can interact with that of the other chromophore, and the excitation energy becomes delocalized over the two chromophores. This dipole–dipole coupling of locally excited states produces a delocalized excitation (called an exciton) and results in a splitting (called exciton splitting) of the locally excited states (Fig. 1). Such interaction is called *exciton coupling* [1] from which stereochemical information may be extracted [1–5], as will be shown in the following.

Exciton Spectra

Exciton coupling is manifested in two distinct bands in the UV-Vis spectrum, one red-shifted from the center of the local excitation, the other blue-shifted. However, unless the exciton splitting is large, a single broad band is more typically seen if both exciton transitions are allowed (Fig. 2). When only one exciton transition is allowed, the absorption spectrum may appear as either a red-shifted or blue-shifted single band. When the interacting chromophores are oriented to form a chiral array, the exciton transitions may be detected by circular dichroism (CD) spectroscopy, with spectra typically taking on a characteristic *bisignate* form. Each of the UV-Vis exciton bands has a corresponding CD band when the two chromophores are arranged in a chiral orientation. Since the CD transitions from an exciton couplet are always oppositely signed, exciton interaction is generally detected much more easily by CD spectroscopy than by UV-Vis spectroscopy. Important for analyzing stereochemistry, the signed order of the bisignate CD spectrum can be correlated with the absolute

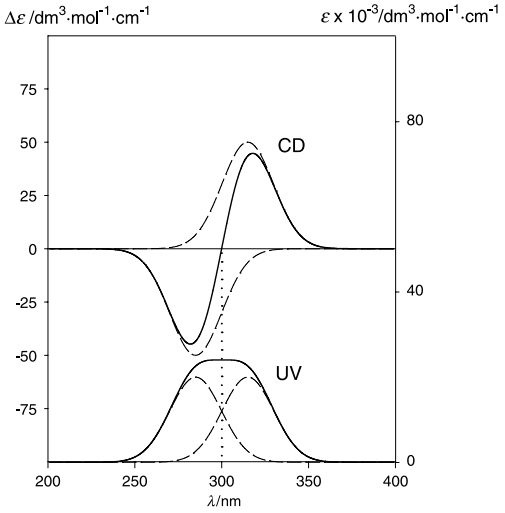

Fig. 2. Exciton coupling detected by simulated UV (lower) and CD (upper) spectroscopy; the observed UV curve comes from summing the UV curves for the two exciton transitions; the observed bisignate CD curve arises from summing the two oppositely-signed CD curves from the two exciton transitions

orientation of the interacting chromophores, according to the *Exciton Chirality Rule* of *Harada* at Tohoku University and *Nakanishi* at Columbia University [2, 3].

Both UV and CD exciton spectra arise from the electronic spectral properties of the component chromophores, the distance between the chromophores and their relative orientation [2, 3, 6]. Because excitons originate in electric transition dipole–dipole coupling, strongly-allowed transitions with large transition dipoles are intrinsically more effective than weakly-allowed transitions, given that dipole–dipole interaction falls off as the inverse cube of the separation distance. Electronic transition intensity and interchromophoric distance are important factors in exciton coupling, as is the relative orientation of the chromophores (specifically, the relative orientation of the relevant transition dipoles). The orientation of two transition dipoles (and chromophores) is important because it determines the allowedness of the two exciton transitions, because it represents stereochemistry and relates absolute stereochemistry to the signed order of the exciton CD couplet. The relative orientation of two dipoles may be broken down into three limiting cases (Fig. 3) that correlate orientation with predicted UV-Vis and CD spectra. Chromophores stacked with transition moments parallel are predicted to exhibit a blue-shifted UV-Vis band because only the higher energy, shorter wavelength exciton transition is allowed [1]. In contrast, chromophores with transition moments in an in-line orientation exhibit a red-shifted UV band because only the lower-energy (longer wavelength) excitation is allowed. In these two limiting cases, the transition dipoles do not form a chiral array; thus no CD results. In the more general orientation (oblique) both exciton transitions are allowed, and the composite UV-Vis band is split or unsplit, depending on whether the exciton splitting energy (V) is large or small. With a chiral oblique orientation one sees a bisignate CD curve, a composite from overlapping positive and negative *Cotton* effects.

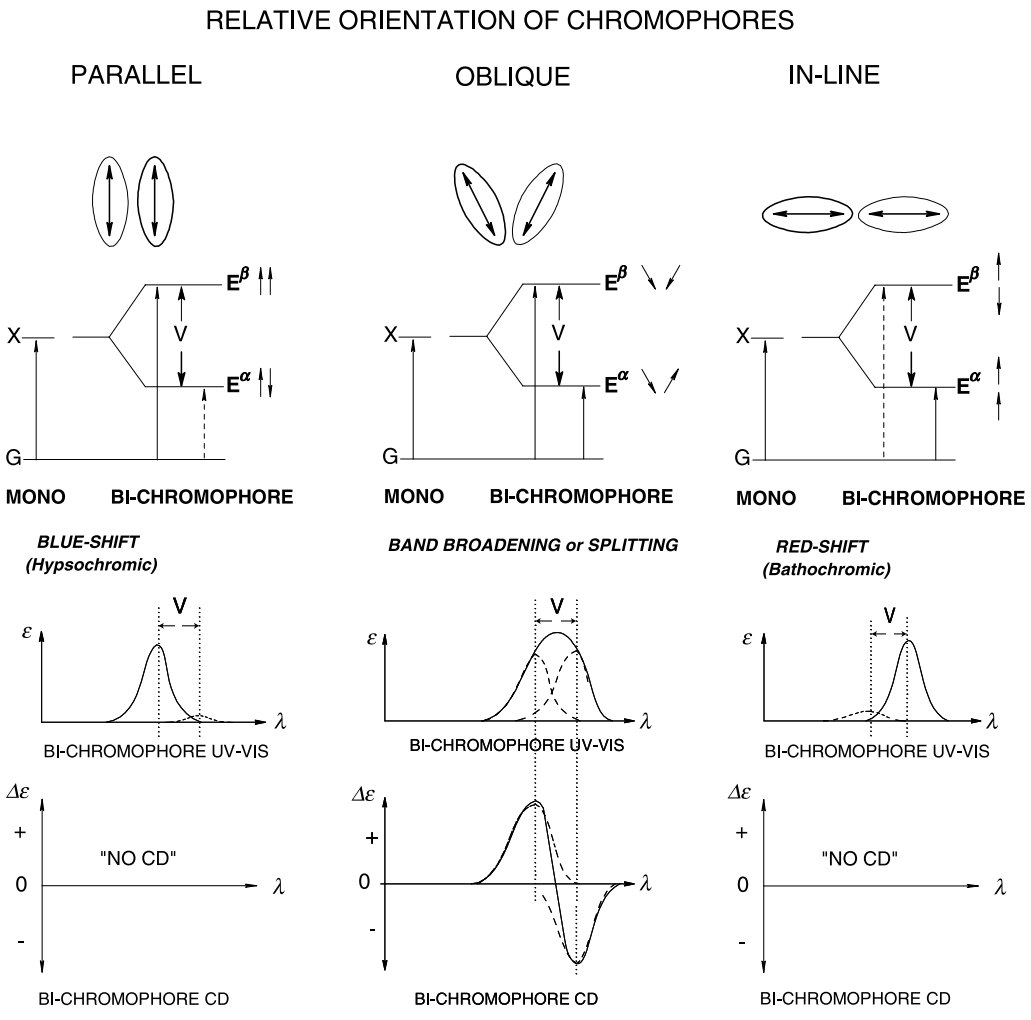

Fig. 3. Orientation dependence in exciton coupling between two chromophores (ellipsoids) and their long-axis transition dipoles (represented by double-headed arrows); the solid single-headed arrows connecting ground (G) and excited (X) states represent allowed transitions; dashed arrows represent forbidden transitions; the consequences of the orientation may be found in wavelength-shifted UV-Vis spectra; two limiting orientations lead to red-shifted (in-line) and blue-shifted (parallel) UV-Vis bands; in the oblique orientation, both transitions are allowed and lead to broadened or split UV-Vis spectra; allowed CD transitions are found only when the dipoles have a chiral, oblique orientation or form a chiral array; V is the exciton splitting

Orientation Dependence of Chromophores in Exciton Coupling UV and CD

A useful example of how orientation dependence affects coupled spectra may be seen clearly in the UV-Vis spectra of bis-porphyrins [7] (Fig. 4). Mono-porphyrin spectra (Fig. 4A) show a typical sharp and narrow, very intense *Soret* band near 400 nm and weak long wavelength bands near 500 nm. When two porphyrin chromophores are present, however (Figs. 4B–4D), the *Soret* band is usually split and shifted, which may be taken as evidence for interchromophoric interaction (exciton

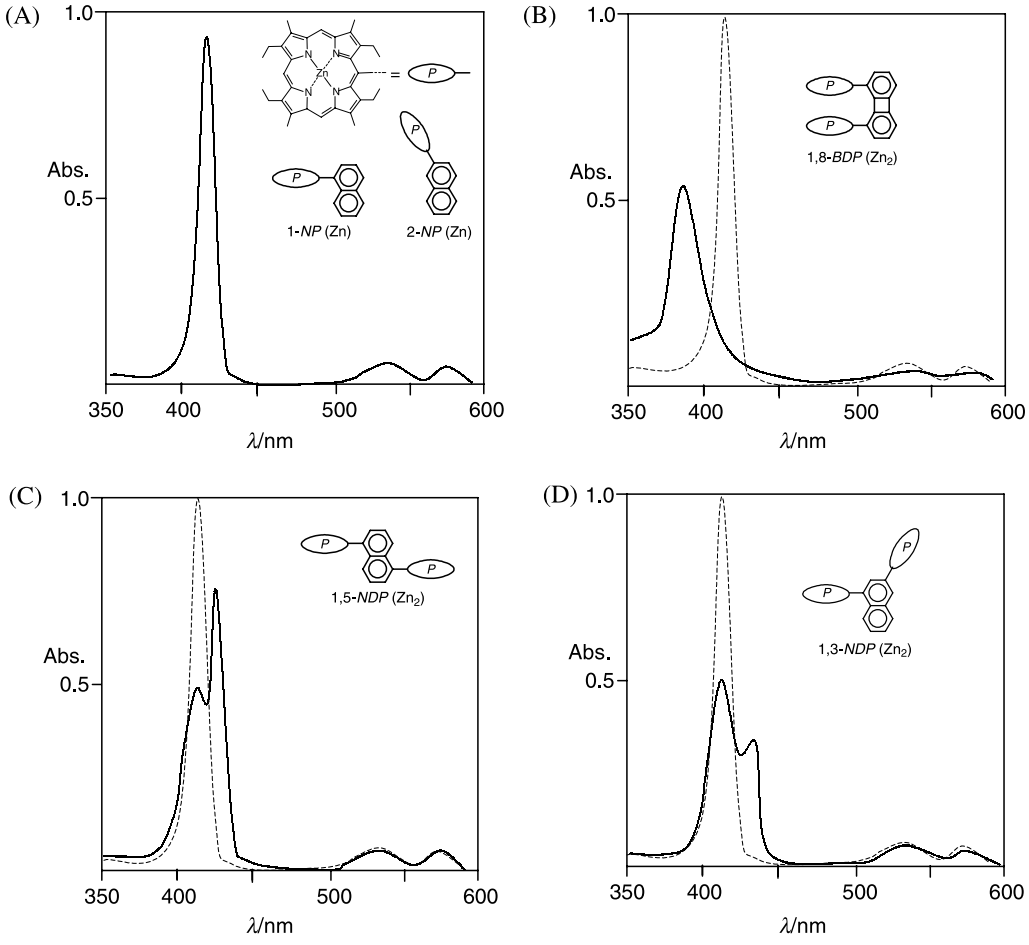

Fig. 4. UV-Vis absorption spectra of zinc etioporphyrins attached covalently to a naphthalene; (A) is the reference spectrum for monomeric 1-naphthyl and 2-naphthyl porphyrins: 1-*NP* and 2-*NP*; (B)–(D) compare the spectra (dashed line) of the monomer porphyrins of (A) to those of variously oriented porphyrin dimers (redrawn from Ref. [7])

coupling). Absent such interaction, the spectra of Figs. 4B–4D would look exactly like that of Fig. 4A, at twice the intensity.

Figures 4B–4D illustrate the dependence of the UV-Vis spectra on the orientation of the two chromophores. When the two porphyrin chromophores lie in a stacked or parallel arrangement (Fig. 4B), a blue-shifted single band is observed, exactly as predicted (Fig. 3, left). The *Soret* band is blue-shifted and broadened relative to the monochromophore. At the other extreme, when the porphyrin chromophores are arranged approximately in-line (Fig. 4C), exciton coupling theory predicts a red-shifted band (Fig. 3, right). In this example, one sees (Fig. 4C) two bands, with the more intense band being red-shifted. The presence of the weak, shorter wavelength band indicates that the transition dipoles are not arranged perfectly in-line. In the oblique orientation of Fig. 4D, two bands are observed, as predicted (Fig. 3, middle). Other examples of exciton-coupling in UV-Vis spectroscopy may be found [1–5], often with splittings not as large as those seen in

Figs. 4B–4D. In such cases, when the chromophores constitute a chiral array, CD can be an excellent tool for detecting and studying exciton coupling [2–5]. Porphyrins are becoming a potent chromophore for adjunct exciton chirality CD and the determination of absolute configuration [3, 4, 8].

Anthracene (***A***) is also a particularly good chromophore for detecting exciton coupling and examining orientation dependence. It has intense UV transitions, hence large electric transition dipole moments: one oriented along its long axis (^1B_b), another oriented along the short axis (^1L_a), as shown in Fig. 5. The more intense (^1B_b, $\varepsilon \sim 200000\,dm^3 \cdot mol^{-1} \cdot cm^{-1}$) is polarized along the long axis of the chromophore; the less intense (^1L_a $\varepsilon \sim 7500\,dm^3 \cdot mol^{-1} \cdot cm^{-1}$) is oriented along the short axis, with dipole strengths of 88×10^{36} and 2.7×10^{36} cgs [2]. In the

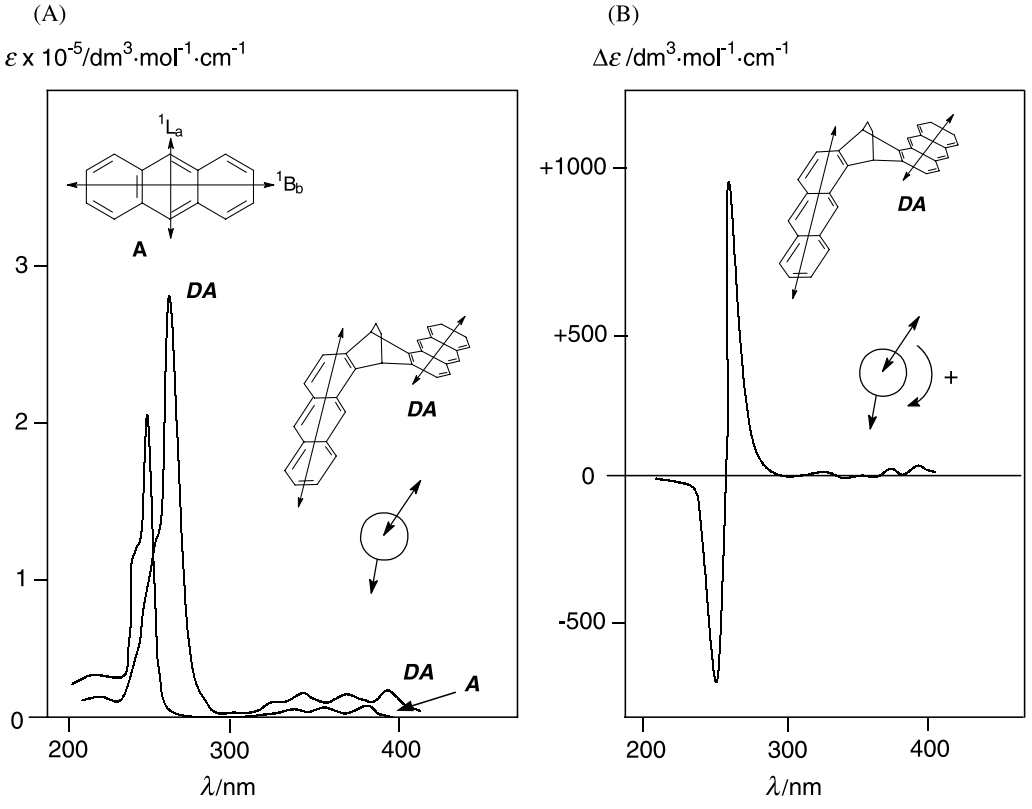

Fig. 5. (A) UV spectra of anthracene (***A***) and the di-anthracene (***DA***) fused to bicyclo[2.2.2]octane; the double-headed arrows (⟷) shown on the structure of ***A*** are the in-plane orientations of the electric dipole transition moment vectors associated with an intense short wavelength UV absorption (^1B_b) near 250 nm and a weak long wavelength absorption (^1L_a) near 360 nm; λ_{max} for the exciton bands of bis-anthracene is red shifted; the absorption λ_{max} of ***DA*** is red-shifted relative to that of ***A*** because the former derives from an exciton interaction where the transition dipoles are oriented approximately in-line (see Fig. 3); (B) CD spectrum of the chiral bis-anthracene (***DA***); the in-plane long-axis oriented electric transition dipoles (⟷) correspond to the ~250 nm UV transition of each ***A*** chromophore and in ***DA*** intersect at a positive torsion angle + ~151°; the signed order of the CD *Cotton* effects of the ~250 nm exciton couplet indicates a (+)-helical orientation of the two electric transition dipoles, confirming the absolute configuration shown (redrawn from Ref. [2])

chiral example (***DA***) of Fig. 5, with anthracenes fused to the bicyclo[2.2.2]octane framework [2], the strong long axis-polarized transition dipoles of the chromophores are not oriented parallel. They lie one in each of two planes that intersect at a dihedral angle of $\sim$120° and intersect nearly in-line at an obtuse angle of $\sim$150°. The UV spectrum of ***DA*** clearly resembles that of its individual component chromophores but differs significantly; 1) It is not simply the sum of two *independent* anthracene transitions, which one would obtain if the two ***A*** chromophores did not interact. 2) Instead, characteristic of two overlapping *exciton* transitions, the ***DA*** spectrum shows a broadened and intensified ^1B_b band that is red-shifted from 252 to 267 nm. Broadening is due to unresolved exciton splitting, and the bathochromic shift is due to an alignment of the ^1B_b transition dipoles approaching in-line: at an $\sim$150° intersection angle.

More noticeable in CD spectroscopy (Fig. 5B), exciton splitting in the ***DA*** seen as a single band in the UV spectrum (Fig. 5A) is seen as oppositely-signed members of a characteristic exciton couplet. The intensity ($\Delta\varepsilon$) of the exciton CD transitions is very large compared to ordinary CD spectra ($|\Delta\varepsilon| \sim 1$ to $10\,dm^3 \cdot mol^{-1} \cdot cm^{-1}$ [5]) from non-interacting chromophores, and the signed order of the exciton couplet CD *Cotton* effects may be correlated with the absolute stereochemistry of the molecule, specifically, with the helicity of the relevant electric dipole transition moments, according to the Exciton Chirality Rule [2–4]. The long-axis transition dipoles make a *positive* dihedral or torsion angle in ***DA*** (Fig. 5B), and a positive torsion angle should correlate with a long-wavelength *positive Cotton* effect of the exciton CD couplet.

The Exciton Chirality Rule and Absolute Configuration

According to the *Harada* and *Nakanishi*'s Exciton Chirality Rule [2–3], when the relevant transition moments are oriented to form a positive (+) torsion angle (*positive chirality*), the long wavelength component of the associated exciton couplet can be expected to exhibit a positive *Cotton* effect (Fig. 6), as found in ***DA*** of Fig. 5B. When they are oriented to form a negative (−) torsion angle (*negative chirality*), the long wavelength *Cotton* effect is negative. The CD spectrum of ***DA*** (Fig. 5B) clearly shows an exciton splitting as two oppositely-signed, very intense *Cotton* effects near 267 nm. The intensity ($\Delta\varepsilon$) surpasses that from dissymmetric vicinal action, indicating that exciton systems might be recognized by very intense bisignate CD *Cotton* effects. The signed order of the *Cotton* effects can be correlated with the relative orientation of the ^1B_b transition moments from the two anthracene chromophores. The extraordinarily intense exciton couplet of ***DA*** has a (+) component at 268 nm and (−) component at 250 nm, thus positive (+) exciton chirality, which predicts a (+) helical orientation of the transition dipoles – as is characteristic of the absolute configuration shown. In general, from analyses of CD (or ORD) spectral data, one can determine the absolute configuration when the conformation is known, and one can obtain information on the conformation when the absolute configuration is known. Exciton CD spectroscopy is typically used to determine absolute configuration. Thus, from an exciton CD spectrum, one can deduce the helical orientation of the transition moments, and with knowledge of the electronic structure and orientation of the relevant electric transition dipoles, one

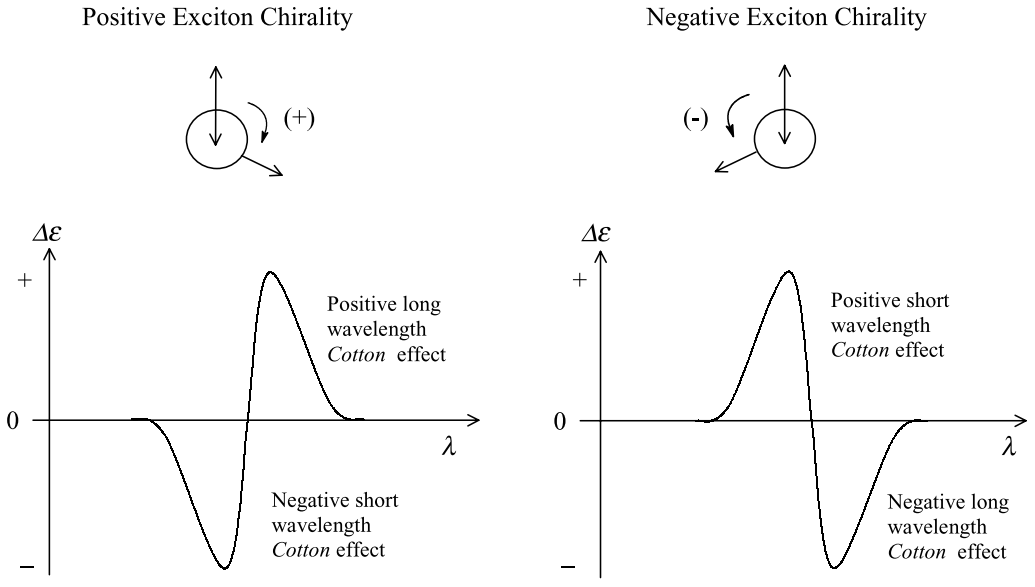

Fig. 6. Graphical illustration of the Exciton Chirality Rule that relates the torsion angle or helicity of two interacting electric dipole transition moments (⟷) to the signed order of the CD *Cotton* effects

can elicit the absolute configuration of the bichromophore system or molecule when the constitutional structure is known.

One may find many examples in which Exciton Chirality Rule is used to determine absolute configuration [2–5]. In most cases, a chiral compound is derivatized to introduce one or more suitable chromophores. Hydroxyl groups are commonly derivatized as esters with acids having appropriate, usually aromatic chromophores. The ideal chromophore would have a very intense UV-Vis electronic transition located in a convenient spectral window, with the orientation of its electric transition moment being well-defined relative to the ester *R*–O bond. 4-Dimethylaminobenzoate, with an intense ($\varepsilon \sim 30000\,\mathrm{dm^3 \cdot mol^{-1} \cdot cm^{-1}}$) transition (dipole oriented along the long axis of the molecule from nitrogen to carboxyl), is an easily accessible chromophore, absorbing in a generally non-interfering UV region (near 310 nm). Although the ester chromophore can adopt a large number of different conformations, the *s-cis* predominates; thus, the relevant transition dipole is typically aligned parallel to the ester O–*R* bond. Consequently, for a 1,2-diol diester the relative helicity (+ or −) of the transition dipoles can be determined by inspection, and one can make an assignment of absolute configuration from the CD spectrum. A good derivatizing agent is thus a symmetric acid in which the alignment of strongly allowed electric dipole transition moment is known with a high degree of certainty [5].

Application of the Exciton Chirality Rule to determine the absolute configuration of *trans*-1,2-cyclohexanediol is straightforward. Assume a chair conformation, which means both OH groups are equatorial. Looking down the C–C bond connecting the carbons bearing the OH groups (Fig. 7), one sees that the O–C–C–O torsion angles have opposite helicities: (+) for the (1*S*,2*S*) enantiomer, (−) for the (1*R*,2*R*). In the bis-4-dimethylaminobenzoate derivative, the relevant electric

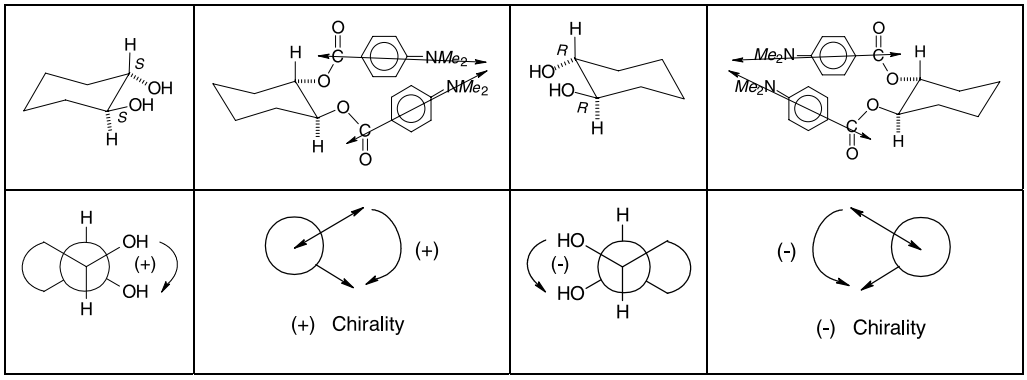

Fig. 7. Conformational structure and *Newman* projection diagrams of (1*S*,2*S*)- and (1*R*,2*R*)-cyclohexanediol and their bis-4-dimethylaminobenzoate derivatives

dipole transition moments align parallel to the C–O bonds of the diol and thus the torsion angle and helicity made by the electric transition dipoles is the same as that of the O–C–C–O torsion angle, with $(+)$ and $(-)$ exciton chirality as above. That is, according to the Exciton Chirality Rule, the (1*S*,2*S*) diester will exhibit a *positive* exciton chirality, with long wavelength positive and short wavelength negative *Cotton* effects for the ~310 nm electronic transition(s), and the (1*R*,2*R*) diester will exhibit a *negative* exciton chirality with a long wavelength negative and short wavelength positive *Cotton* effects (Fig. 7).

As may be seen in Fig. 8, the bis-4-dimethylaminobenzoate ester of (1*S*,2*S*) and (1*R*,2*R*)-cyclohexanediol exhibit a broadened UV spectrum, with a nearly split long wavelength absorption near 310 nm, lying between the components of the

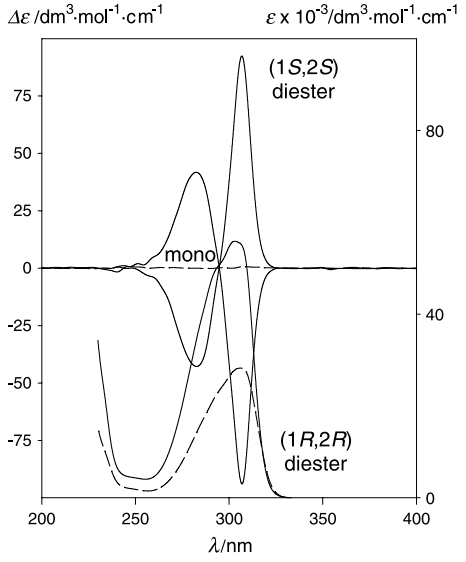

Fig. 8. CD (————) and UV (————) spectra of (1*R*,2*R*)- and (1*S*,2*S*)-cyclohexanediol bis-4-dimethylaminobenzoate; CD (- - - - - - - -) and UV (- - - - - - - -) spectra of mono-4-dimethylaminobenzoate in cyclohexane solvent at 22°C

CD couplets, as predicted from Figs. 2 and 3. Mirror image bisignate exciton CD curves are seen, and the signed order of each couplet correlates with the helicity of the diol O–C–C–O torsion angle and, more exactly, with the transition moments of the diester, consistent with the predictions of the Exciton Chirality Rule. The CD spectrum of the mono ester (mono, Fig. 8) is very different and shows an extremely weak monosignate curve. Clearly, the presence of two 4-dimethylaminobenzoate chromophores makes an enormous difference: the diester spectra are seen to be neither the sum of two identical mono-ester UV curves, which would be coincident and not broadened or shifted (Fig. 3), or two identical CD curves, which would be net mono-signate. A striking contrast that implies a different origin for the diester transitions – one diagnostic for and consistent with exciton coupling.

Part B. Exciton CD from Fluorescent Dipyrrinones

Introduction

A few years ago, we showed that the yellow dipyrrinone chromophore (Fig. 9), with its intense long wavelength π–π^* absorption ($\varepsilon_{max} \sim 30000\,dm^3 \cdot mol^{-1} \cdot cm^{-1}$, $\lambda_{max} \sim 410\,nm$) electric transition dipole moment oriented along the long axis of the molecule [9, 10] can be an effective chromophore for exciton chirality CD studies in the visible region [11]. Positions C(2) and C(8) lie approximately along the long axis of the molecule and thus constitute appropriate sites for attachment to chiral molecules such as 1,2-cyclohexanediol. In the earlier studies we compared exciton CD spectra of 1,2-cyclohexanediol and 1,2-diaminocyclohexane derivatives with dipyrrinones with acetic acid and propionic acid belts attached to C(8). The shorter belt, with fewer degrees of motional freedom, gave the more intense CD, and both acetic and propionic derivatives correlated well with the Exciton Chirality Rule [11]. However, we could not prepare a derivative with the carboxylic acid group attached directly to C(8) and thereby reduce the conformational mobility.

More recently we showed that dipyrrinones with a carbonyl bridge between the pyrrole and lactam are highly fluorescent, with fluorescence quantum yields $\phi_F > 0.5$ [12]. Strong fluorescence arises by preventing the energy-wasting $4Z \rightarrow 4E$ dipyrrinone carbon–carbon double bond isomerization [13]. For those

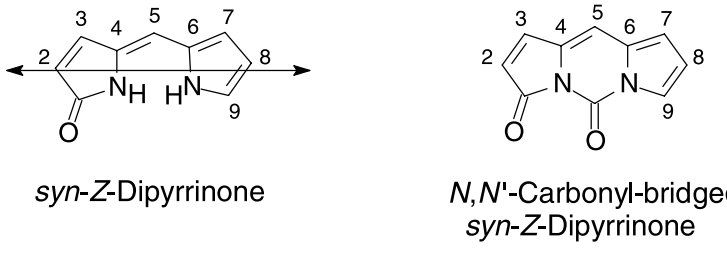

Fig. 9. (Left) The 10*H*-dipyrrin-1-one chromophore in its *syn* conformation with the approximate orientation of the long wavelength (~410 nm) electric transition dipole moment (⟷); (Right) the highly fluorescent *N*,*N*′-carbonyl-bridged dipyrrinone chromophore (dipyrrolo[1,2-c:2′,1′-f]pyrimidine-3,5-dione), with dipyrrinone numbering systems

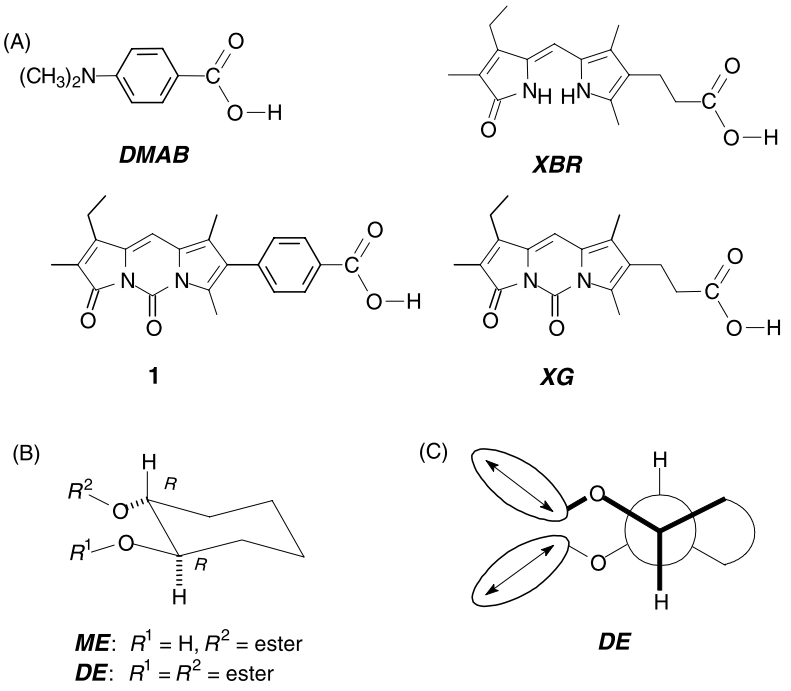

Fig. 10. (A) The chromophores of this work: 4-dimethylaminobenzoic acid (***DMAB***), xanthobilirubic acid (***XBR***), fluorescent xanthoglow (***XG***), and its benzoic acid analog **1**; (B) (1*R*,2*R*)-cyclohexanediol ($R^1 = R^2 = H$) and its mono- and di-esters (***ME*** and ***DE***) with the chromophoric carboxylic acids of (A); (C) *Newman* drawing looking down the 1,2 carbon-carbon bond of the diol derivatized as a diester (***DE***) with the chromophores of (A)

studies [12] we prepared a derivative of xanthobilirubic acid (***XBR***, Fig. 10A), which we call xanthoglow (***XG***, Fig. 10A). To extend our dipyrrinone chromophore stereochemical investigations into exciton CD of *fluorescent* chromophores, we prepared a new fluorescent dipyrrinone derivative (**1**), with fewer orientational degrees of freedom than ***XG***, a benzoic acid replacing propionic at C(8). With the carboxyl group attached to a rigid benzene ring spacer at C(8), the dipyrrinone long wavelength transition moment is expected to lie approximately parallel to the long axis of the benzoic acid. In the current study, we prepared cyclohexanediol esters with ***XG*** and **1** and compared the CD of mono- and di-esters (***ME*** and ***DE***) of ***XBR***, ***XG***, and **1** with optically active 1,2-cyclohexanediol (Fig. 10B). Although a fluorescent chromophore is not required for exciton chirality absorption CD studies, a strongly fluorescent chromophore might open up the possibility for complementary CD studies in the emission mode, where increased sensitivity (from very low sample concentrations) could be an advantage.

Results and Discussion

Synthesis Aspects

Xanthoglow (***XG***, Fig. 10A) was known from earlier studies; its benzoic acid analog **1** was prepared as outlined in the Scheme. The known dipyrrinone **2**

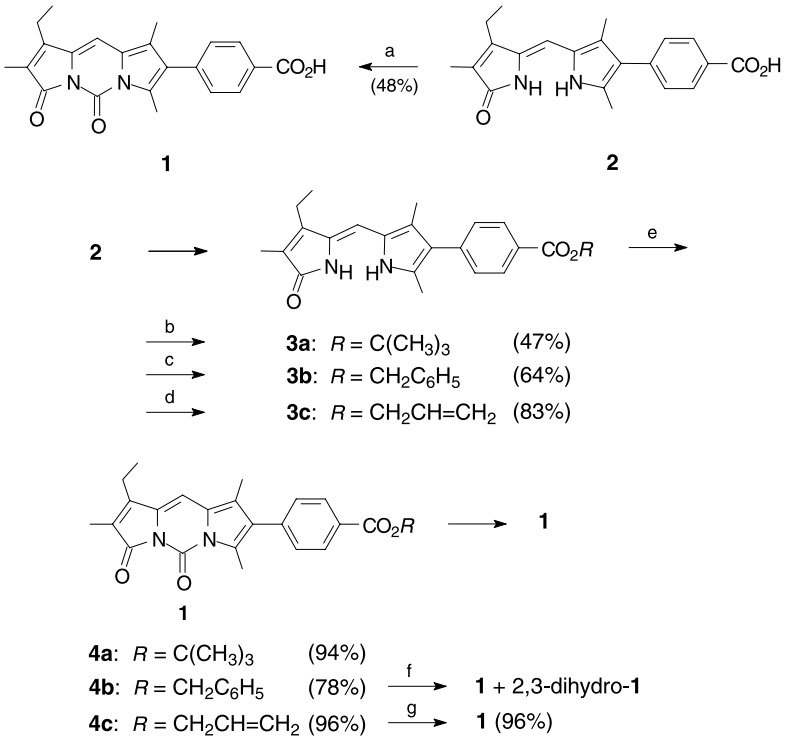

a: *CDI*, *DBU*, then aq HCl; b: *CDI*, *DBU*, $(CH_3)_3COH$ or $(CH_3)_3COH + MgSO_4/H_2SO_4$;

c: $BrCH_2C_6H_5 + Cs_2CO_3$; d: $BrCH_2CH{=}CH_2 + Cs_2CO_3$; e: *CDI*, *DBU*; f: H_2/Pd(C);

g: $Pd[PPh_3]_4$, pyrrolidine

Scheme

[14], which is rather insoluble in most organic solvents served as the starting material, and procedures for converting it to **1** were investigated. Direct reaction with 1,1′-carbonyldiimidazole (*CDI*) works best with esters, although conditions were recently developed to convert acid **2** into **1** in moderate yield after mild hydrolysis of the intermediate acyl imidazole. To react an ester with *CDI*, an appropriate ester had to be chosen so as to facilitate conversion of the *N*,*N*′-carbonyl-bridged dipyrrinone ester to its acid **1** without loss of the carbonyl bridge. Saponification of the methyl or ethyl ester of **1** proved unsatisfactory; so, more easily removed acid protecting groups were investigated: *tert*-butyl and benzyl. Conversion of **2** to its *tert*-butyl ester **3a** by activation of the acid with *CDI* then treatment with *tert*-butyl alcohol gave only a 27% yield of **3a**, but (on a small scale) the yield could be improved to 47% by esterifying in the presence of sulfuric acid adsorbed onto anhydrous magnesium sulfate [15]. Attempts to scale up the reaction led to lower yields. Thus, although the *tert*-butyl ester **3a** could be converted to the *N*,*N*′-carbonyl-bridged dipyrrinone **4a**, we abandoned using the acid-sensitive *tert*-butyl protecting group in favor of the hydrogenolyzable benzyl

protecting group. Thus, reaction of **2** with cesium carbonate followed by benzyl bromide afforded **3b** in 64% yield, and **3b** was smoothly converted to **4b** in 78% yield. However, deprotection of **4b** led to both **1** as well as its 2,3-dihydro analog, and this procedure, too, was abandoned in favor of a more successful route using the allyl protecting group. Thus, the cesium carboxylate of **2** was reacted with allyl bromide to give **3c** in 83% yield, and **3c** was converted to **4c** in 96% yield. Deprotection of **4c** using tetrakis(triphenylphosphine)palladium(0) and pyrrolidine [16] afforded **1** in 96% yield. Conversion of **1** to the di- and mono-esters of (1*S*,2*S*) and (1*R*,2*R*)-cyclohexanediol was accomplished using procedures developed earlier [11] and modified for the current work.

Circular Dichroism

Consistent with an earlier report [11b], the circular dichroism (CD) spectrum of ***XBR-DE*** (Fig. 11) in CH_2Cl_2 clearly shows a negative chirality ($\Delta\varepsilon = -16.0\,\mathrm{dm^3 \cdot mol^{-1} \cdot cm^{-1}}$, $\lambda = 439\,\mathrm{nm}$; $\Delta\varepsilon = +22.3\,\mathrm{dm^3 \cdot mol^{-1} \cdot cm^{-1}}$, $\lambda = 382\,\mathrm{nm}$) exciton transition – as predicted from the Exciton Chirality Rule [2, 3] and simple molecular models. In the same solvents, the *N*,*N*′-carbonyl-bridged dipyrrinone analog (***XG-DE***) also shows a negative chirality exciton CD spectrum, but of a clearly weaker magnitude: $\Delta\varepsilon = -5.2\,\mathrm{dm^3 \cdot mol^{-1} \cdot cm^{-1}}$, $\lambda = 433\,\mathrm{nm}$; $\Delta\varepsilon = +2.4\,\mathrm{dm^3 \cdot mol^{-1} \cdot cm^{-1}}$, $\lambda = 394\,\mathrm{nm}$ (Fig. 11). Thus, ***XG*** would appear to be a poor substitute for ***XBR*** as an exciton coupling chromophore. More optimistically for circularly polarized luminescence (CPL) or fluorescence detected CD (FDCD), ϕ_F of ***XG-DE*** remained high: $\phi_F = 0.37$ ($CHCl_3$).

Suspecting that by stiffening the linker between the chromophore enhanced CD intensities would be found, we used **1** to prepare and examine **1**-***DE***. The reasoning

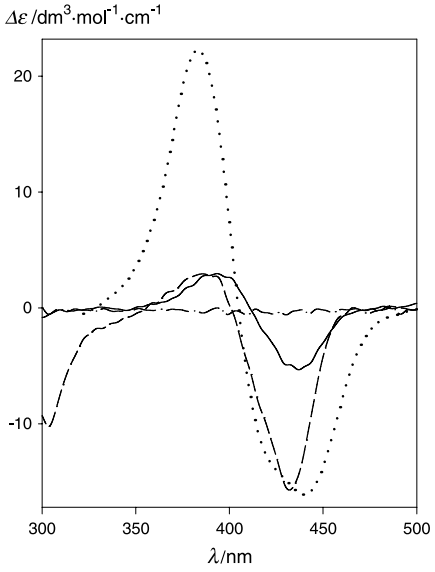

Fig. 11. CD spectra in CH_2Cl_2 of ***XBR-DE*** (· · · ·), ***XG-DE*** (———), **1**-***DE*** (- - - -), and **1**-***ME*** (– · – ·) at room temperature

Table 1. Comparison of the circular dichroism and UV-Vis spectral data[a] from the esters of (1*R*,2*R*)-cyclohexanediol with **1**, ***XG***, and ***XBR***

Diester of	Solvent	Circular dichroism		
		$\Delta\varepsilon_{1\ max}$ (λ_1)	λ at $\Delta\varepsilon = 0$	$\Delta\varepsilon_{2\ max}$ (λ_2)
1	cyclohexane	−19.0 (429)	400	+8.8 (380)
XG		−5.1 (443)	411	+5.1 (394)
1	benzene	−17.4 (431)	401	+3.9 (381)
XG		−3.8 (442)	416	+3.4 (388)
XBR[c]		−13.6 (445)	409	+18.9 (386)
1	$CHCl_3$	−15.2 (432)	403	+3.9 (380)
XG		−5.2 (438)	411	+2.6 (393)
1	CH_2Cl_2	−15.3 (431)	400	+3.6 (380)
XG		−4.6 (437)	410	+2.2 (396)
XBR[c]		−16.0 (439)	404	+22.3 (382)
1	CH_3CN	−17.2 (426)	394	+4.0 (388)
XG		−3.1 (436)	411	+2.0 (398)
1	CH_3OH	−16.7 (429)	402	+6.3 (381)
XG		−2.4 (451)	425	+3.0 (401)
1	$(CH_3)_2SO$	−15.1 (432)	400	+3.4 (380)
XG		−3.0 (438)	410	+2.4 (397)
XBR[c]		−12.6 (419)	397	+6.7 (382)

Diester of	Solvent	UV-Vis			
		ε_{max} (λ)	ε_{max} (λ)	ε_{max} (λ)[b]	ε_{max} (λ)[b]
1	cyclohexane	38200 (429)	41000 (407)	22500 (430)	22700 (409)
XG		25800 (434)[sh]	34100 (409)	19200 (432)	19200 (412)
1	benzene	40600 (428)[sh]	41100 (416)	20800 (425)	20900 (417)
XG		29100 (434)[sh]	33900 (413)	18400 (428)	18200 (417)[sh]
XBR[c]			61400 (393)		
1	$CHCl_3$		42200 (421)	21000 (424)	
XG		32300 (435)[sh]	34300 (421)	18800 (427)	
1	CH_2Cl_2		42600 (421)	21500 (421)	
XG		34100 (434)[sh]	36000 (421)	19200 (426)	
XBR[c]			61400 (389)		26700 (400)
1	CH_3CN		43000 (415)	21600 (417)	
XG		31500 (430)[sh]	34600 (414)	19100 (421)	
1	CH_3OH		40600 (420)	21000 (421)	
XG			32600 (417)	18300 (426)	
1	$(CH_3)_2SO$		41000 (421)	20700 (421)	
XG			34000 (419)	18900 (427)	
XBR[c]			51900 (408)		

[a] ε and $\Delta\varepsilon$ in $dm^3 \cdot mol^{-1} \cdot cm^{-1}$, λ in nm; [b] data for the mono-ester; [c] data from Ref. [11b]

was at least qualitatively correct, as **1**-***DE*** gave an exciton CD spectrum (Fig. 11) with $\Delta\varepsilon = -15.6\,dm^3 \cdot mol^{-1} \cdot cm^{-1}$ ($\lambda = 431$ nm); $\Delta\varepsilon = +3.7\,dm^3 \cdot mol^{-1} \cdot cm^{-1}$ ($\lambda = 383$ nm), with the CD intensities being closer to those observed for ***XBR-DE***.

Table 2. Fluorescence quantum yields (ϕ_F) of monoesters (***ME***) and Diesters (***DE***) of **1** and ***XG*** with *trans*-1,2-cyclohexanediol

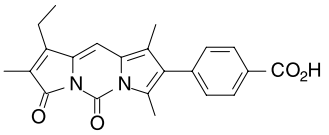

1

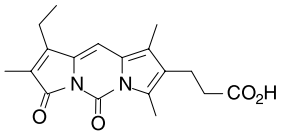

XG

	ϕ_F[a]		ϕ_F	
Solvent[b]	**1**-***ME*** (λ_{em}) [c]	**1**-***DE*** (λ_{em})	***XG*-*ME*** (λ_{em})	***XG*-*DE*** (λ_{em})
Cyclohexane	0.77 (458)	0.47 (473)	0.64 (474)	0.15 (501)
Benzene	0.76 (483)	0.62 (481)	0.74 (487)	0.18 (501)
Chloroform	0.65 (492)	0.59 (493)	0.68 (497)	0.37 (501)
Methanol	0.40 (526)	0.17 (524)	0.34 (530)	0.15 (509)
Dimethyl sulfoxide	0.66 (504)	0.43 (503)	0.65 (506)	0.13 (507)

[a] Relative quantum yield determined (Ref. [17]) *vs.* 9,10-diphenylanthracene standard: $\phi_F = 0.90$ in cyclohexane; [b] concentration 6.4×10^{-7} to 1.2×10^{-6} mol · dm^{-3}; [c] emission wavelength at maximum intensity

Although the CD intensities of **1**-***DE*** were disappointingly low, the data for **1**-***DE*** and ***XG*-*DE*** suggest an attenuation due to large distances between the chromophores and/or multiple conformations. Consistent with fluorescence measurements reported for the methyl ester of ***XG*** ($\phi_F = 0.67$, $\lambda_{em} = 497$ nm, $\lambda_{ex} = 419$ nm, $CHCl_3$) [17] and the isobutyl ester of **1** ($\phi_F = 0.66$, $\lambda_{em} = 493$ nm, $\lambda_{ex} = 420$ nm, $CHCl_3$) [18], the fluorescence quantum yields of the mono esters of **1** and ***XG*** with 1,2-cyclohexanediol are also comparably large (Table 2). In the diesters, as might be expected, the ϕ_F values drop, for ***XG*-*DE*** down to about 25–50% of the ϕ_F values from ***XG*-*ME***. Unexpectedly but gratifyingly, the drop is far smaller with the more rigid diester, **1**-***DE***. A comparison of the solvent dependence of ϕ_F from **1**-***DE*** and ***XG*-*DE*** (Table 2) indicates that the ϕ_F values of the former remain much higher than those of the latter, often comparable to those of **1**-***ME***. For example, $\phi_F = 0.59$ ($CHCl_3$) for **1**-***DE***, or some 50% higher than ϕ_F (0.37) from ***XG*-*DE***, thus indicating that **1**-***DE*** might be a worthy candidate for investigations of CPL or FDCD.

Experimental

Nuclear magnetic resonance spectra were measured on a Varian Unity Plus spectrometer at 11.75 T magnetic field strength operating at ^{1}H frequency of 500 MHz and ^{13}C frequency of 125 MHz. Unless otherwise noted, $CDCl_3$ solvent was used throughout, and chemical shifts are reported in δ ppm referenced to residual $CHCl_3$ ^{1}H signal at 7.26 ppm and $CDCl_3$ ^{13}C signal at 77.00 ppm. *J*-modulated spin-echo (Attached Proton Test) and gHMBC experiments were used to assign the ^{13}C NMR signals. All UV-Vis spectra were recorded on a Perkin Elmer Lambda 12 spectrophotometer and the circular dichroism spectra were recorded on a JASCO J-600 dichrograph. The fluorescence spectra were measured on a Jobin Yvon FluoroMax 3 instrument, and quantum yields were determined according to literature procedures [17]. All optical spectral measurements were carried out using 1 cm quartz

cells. Radial chromatography was carried out on Merck silica gel PF_{254} with $CaSO_4$ binder preparative layer grade, using a Chromatotron (Harrison Research, Inc., Palo Alto, CA) with 1, 2, or 4 mm thick rotors and analytical thin-layer chromatography was carried out on J. T. Baker silica gel IB-F plates (125 μm layers). Melting points were determined on a Mel-Temp capillary apparatus and are uncorrected. The combustion analyses for carbon, hydrogen, and nitrogen were carried out by Desert Analytics, Tucson, AZ, and gave results within $\pm 0.3\%$ of the theoretical values. Commercial reagents were used as received from Acros or Aldrich. The solvents for optical spectroscopy were HPLC grade and were distilled under a stream of argon just prior to use. Before the distillation, $CHCl_3$ was passed through a basic alumina column. Dimethyl sulfoxide was distilled at 0.5 mm Hg vacuum collecting the solvent at 0°C and thawing it under Ar. Dipyrrinone **2** was available from previous work [14].

8-[4-(t-Butyloxycarbonyl)phenyl]-3-ethyl-2,7,9-trimethyl-1,10-dihydro-11H-dipyrrin-1-one (**3a**, $C_{25}H_{30}N_2O_3$)

To a vigorously stirred suspension of 4.8 g anhydrous $MgSO_4$ (40 mmol) in 40 cm^3 anhydrous CH_2Cl_2 was slowly added conc H_2SO_4 (0.55 cm^3, 10 mmol) and the mixture was stirred for 20 min [15]. Then 175 mg acid **2** (0.5 mmol) were added followed by 4.8 cm^3 *t*-butanol (50 mmol) and the mixture was stirred in a tightly closed flask for 19 h. Saturated aqueous $NaHCO_3$ solution was added slowly until effervescence ceased and the mixture was partitioned between 200 cm^3 H_2O and 150 cm^3 $CHCl_3$. The organic layer was washed with H_2O (2×100 cm^3), then dried (Na_2SO_4), filtered, and the solvent was evaporated under vacuum. The residue was purified by radial chromatography followed by recrystallization from CH_2Cl_2–CH_3OH. Yield 95 mg (47%); mp 275–279°C (dec); ^{1}H NMR: $\delta = 1.20$ (t, $J = 7.6$ Hz, 3H), 1.62 (s, 9H), 1.96 (s, 3H), 2.19 (s, 3H), 2.49 (s, 3H), 2.57 (q, $J = 7.6$ Hz, 2H), 6.21 (s, 1H), 7.34 (m, $J = 8.1$ Hz, 2H), 8.04 (m, $J = 8.1$ Hz, 2H), 10.66 (br.s, 1H), 11.40 (br.s, 1H) ppm; ^{13}C NMR: $\delta = 8.6$, 10.4, 12.4, 15.0, 18.0, 28.2, 80.8, 100.9, 122.9, 123.0, 123.2, 123.7, 127.9, 129.29, 129.32, 129.5, 132.0, 140.4, 148.5, 165.9, 174.3 ppm.

8-[4-(Benzyloxycarbonyl)phenyl]-3-ethyl-2,7,9-trimethyl-1,10-dihydro-11H-dipyrrin-1-one (**3b**, $C_{28}H_{28}N_2O_3$)

A mixture of 0.70 g dipyrrinone **2** (2.0 mmol), 0.57 g Cs_2CO_3 (1.7 mmol), 15 cm^3 anhydrous dimethylformamide, and 0.7 cm^3 benzyl bromide (6.0 mmol) was stirred under Ar at 50°C for 4 h. After cooling, the mixture was partitioned between 150 cm^3 $CHCl_3$ and 100 cm^3 1% aq HCl. The organic layer was washed with 4×100 cm^3 H_2O, then dried (Na_2SO_4), filtered, and the solvent was evaporated under vacuum. The residue was purified by radial chromatography followed by recrystallization from CH_2Cl_2–CH_3OH. Yield 0.56 g (64%); mp 273–275°C (dec); ^{1}H NMR: $\delta = 1.20$ (t, $J = 7.7$ Hz, 3H), 1.96 (s, 3H), 2.19 (s, 3H), 2.49 (s, 3H), 2.58 (q, $J = 7.7$ Hz, 2H), 5.40 (s, 2H), 6.21 (s, 1H), 7.36 (m, 3H), 7.40 (m, 2H), 7.47 (m, $J = 8.3$ Hz, 2H), 8.12 (m, $J = 8.3$ Hz, 2H), 10.64 (br.s, 1H), 11.36 (br.s, 1H) ppm; ^{13}C NMR: $\delta = 8.6$, 10.4, 12.5, 15.0, 18.0, 66.6, 100.9, 122.7, 123.1, 123.2, 123.6, 127.3, 128.0, 128.1, 128.2, 128.6, 129.6, 129.7, 132.1, 136.2, 141.1, 148.6, 166.5, 174.3 ppm.

8-[4-(Allyloxycarbonyl)phenyl]-3-ethyl-2,7,9-trimethyl-1,10-dihydro-11H-dipyrrin-1-one (**3c**, $C_{24}H_{26}N_2O_3$)

A mixture of 1.75 g dipyrrinone **2** (5.0 mmol), 1.63 g Cs_2CO_3 (5.0 mmol), 30 cm^3 anhydrous dimethylformamide, and 1.3 cm^3 allyl bromide (15.0 mmol) was stirred under Ar in a tightly closed flask at 80–85°C for 16 h. After cooling, the mixture was partitioned between 300 cm^3 $CHCl_3$ and 100 cm^3 1% aq HCl. The organic layer was washed with 4×100 cm^3 H_2O, then dried (Na_2SO_4), filtered, and the solvent was evaporated under vacuum. The residue was purified by radial chromatography followed by recrystallization from CH_2Cl_2–CH_3OH. Yield 1.63 g (83%); mp 280–282° (dec); ^{1}H NMR: $\delta = 1.20$

(t, $J = 7.7$ Hz, 3H), 1.96 (s, 3H), 2.20 (s, 3H), 2.50 (s, 3H), 2.57 (q, $J = 7.7$ Hz, 2H), 4.85 (ddd, $^3J = 5.7$ Hz, $^4J = 1.5$, 1.4 Hz, 2H), 5.31 (ddt, $^3J = 10.4$ Hz, $^4J = 1.4$ Hz, $^2J = 1.2$ Hz, 1H), 5.44 (ddt, $^3J = 17.2$ Hz, $^4J = 1.5$ Hz, $^2J = 1.2$ Hz, 1H), 6.07 (ddt, $J = 17.2$, 10.4, 5.7 Hz, 1H), 6.21 (s, 1H), 7.36 (m, $J = 8.3$ Hz, 2H), 8.11 (m, $J = 8.3$ Hz, 2H), 10.66 (br.s, 1H), 11.39 (br.s, 1H) ppm; ^{13}C NMR: $\delta = 8.5$, 10.4, 12.4, 15.0, 17.9, 65.4, 100.8, 118.1, 122.6, 123.0, 123.2, 123.6, 127.3, 127.9, 129.53, 129.54, 132.1, 132.4, 141.0, 148.5, 166.3, 174.2 ppm.

*General Procedure for N,N-Cyclization Leading to **4a–4c***

A mixture of 1 mmol of dipyrrinone **3a**–**3c**, 0.81 g 1,1′-carbonyldiimidazole (5 mmol), 0.75 cm^3 1,8-diazabicyclo[5.4.0]undec-7-ene (5 mmol), and 80 cm^3 anhydrous CH_2Cl_2 was heated under N_2 at reflux for 16 h. After cooling, the mixture was washed with 1% aq HCl (2×70 cm^3), then with H_2O (3×70 cm^3), and the solution was dried ($MgSO_4$). After filtration and evaporation of the solvent under vacuum, the residue was purified by radial chromatography followed by recrystallization from ethyl acetate-hexane to afford bright yellow tricyclic compounds **4a**–**4c**.

8-[4-(t-Butyloxycarbonyl)phenyl]-1-ethyl-2,7,9-trimethyl-3H,5H-dipyrrolo[1,2-c:2′,1′-f]pyrimidine-3,5-dione (**4a**, $C_{26}H_{28}N_2O_4$)

Yield 0.41 g (94%); mp 201–202°C; ^{1}H NMR: $\delta = 1.23$ (t, $J = 7.7$ Hz, 3H), 1.61 (s, 9H), 1.98 (s, 3H), 2.09 (s, 3H), 2.56 (q, $J = 7.7$ Hz, 2H), 2.65 (s, 3H), 6.46 (s, 1H), 7.29 (m, $J = 8.4$ Hz, 2H), 8.05 (m, $J = 8.4$ Hz, 2H) ppm; ^{13}C NMR: $\delta = 8.5$, 9.7, 13.76, 13.82, 18.0, 28.2, 81.1, 97.0, 119.7, 126.6, 126.7, 129.3, 129.5, 129.9, 130.8, 130.9, 131.9, 138.0, 143.4, 146.6, 165.6, 167.7 ppm.

8-[4-(Benzyloxycarbonyl)phenyl]-1-ethyl-2,7,9-trimethyl-3H,5H-dipyrrolo[1,2-c:2′,1′-f]pyrimidine-3,5-dione (**4b**, $C_{29}H_{26}N_2O_4$)

Yield 0.36 g (78%); mp 177–178°C; ^{1}H NMR: $\delta = 1.23$ (t, $J = 7.7$ Hz, 3H), 1.97 (s, 3H), 2.09 (s, 3H), 2.56 (q, $J = 7.7$ Hz, 2H), 2.65 (s, 3H), 5.39 (s, 2H), 6.46 (s, 1H), 7.32 (m, $J = 8.4$ Hz, 2H), 7.35 (m, 1H), 7.40 (m, 2H), 7.46 (m, 2H), 8.14 (m, $J = 8.4$ Hz, 2H) ppm; ^{13}C NMR: $\delta = 8.5$, 9.7, 13.76, 13.80, 18.0, 66.7, 96.9, 119.6, 126.66, 126.68, 128.1, 128.2, 128.6, 128.8, 129.1, 129.8, 130.0, 130.9, 131.9, 136.0, 138.7, 143.4, 146.6, 166.2, 167.6 ppm.

8-[4-(Allyloxycarbonyl)phenyl]-1-ethyl-2,7,9-trimethyl-3H,5H-dipyrrolo[1,2-c:2′,1′-f]pyrimidine-3,5-dione (**4c**, $C_{25}H_{24}N_2O_4$)

Yield 0.40 g (96%); mp 195–196°C; ^{1}H NMR: $\delta = 1.24$ (t, $J = 7.7$ Hz, 3H), 1.98 (s, 3H), 2.10 (s, 3H), 2.57 (q, $J = 7.7$ Hz, 2H), 2.66 (s, 3H), 4.85 (ddd, $^3J = 5.7$ Hz, $^4J = 1.5$, 1.4 Hz, 2H), 5.30 (ddt, $^3J = 10.4$ Hz, $^4J = 1.4$ Hz, $^2J = 1.2$ Hz, 1H), 5.43 (ddt, $^3J = 17.3$ Hz, $^4J = 1.5$ Hz, $^2J = 1.2$ Hz, 1H), 6.05 (ddt, $J = 17.3$, 10.4, 5.7 Hz, 1H), 6.46 (s, 1H), 7.32 (m, $J = 8.5$ Hz, 2H), 8.13 (m, $J = 8.5$ Hz, 2H) ppm; ^{13}C NMR: $\delta = 8.4$, 9.6, 13.70, 13.73, 17.9, 65.5, 96.9, 118.2, 119.6, 126.5, 126.6, 128.8, 129.0, 129.6, 129.9, 130.8, 131.8, 132.1, 138.5, 143.3, 146.5, 165.9, 167.5 ppm.

8-(4-Carboxyphenyl)-1-ethyl-2,7,9-trimethyl-3H,5H-dipyrrolo[1,2-c:2′,1′-f]pyrimidine-3,5-dione (**1**, $C_{22}H_{20}N_2O_4$)

To an Ar-protected suspension of 1.67 g allyl ester **4c** (4.0 mmol) in 25 cm^3 anhydrous acetonitrile was added 0.23 g tetrakis(triphenylphosphine)palladium(0) (0.2 mmol) and 0.10 g triphenylphosphine (0.4 mmol), followed by a solution of 0.37 cm^3 pyrrolidine (4.4 mmol) in 3 cm^3 acetonitrile, and the mixture was stirred for 6 h [16]. Then it was diluted with 400 cm^3 CH_2CH_2:$CHCl_3$ ~ 1:1 (by volume) and washed with 1% aq HCl (2×50 cm^3) and H_2O (2×100 cm^3). After drying (Na_2SO_4), filtration, and

evaporation of the solvents under vacuum, the residue was triturated with benzene (30 cm^3) and the product was separated by filtration. Washing with 2×5 cm^3 benzene afforded acid **1** with sufficient purity for use in the next steps. Small portion of the crude product was purified by radial chromatography followed by recrystallization from ethyl acetate-hexane to give analytically pure acid **1**. Yield 1.44 g (96%); mp 319–321°C; ^{1}H NMR (*DMSO*-d_6): $\delta = 1.13$ (t, $J = 7.6$ Hz, 3H), 1.86 (s, 3H), 2.09 (s, 3H), 2.54 (s, 3H), 2.59 (q, $J = 7.6$ Hz, 2H), 7.11 (s, 1H), 7.40 (m, $J = 8.3$ Hz, 2H), 8.00 (m, $J = 8.3$ Hz, 2H), 12.96 (br.s, 1H) ppm; ^{13}C NMR (*DMSO*-d_6): $\delta = 8.1$, 9.4, 13.6, 13.7, 17.2, 98.1, 119.3, 125.4, 126.9, 128.3, 129.3, 129.4, 129.9, 130.5, 130.6, 137.8, 142.5, 147.3, 166.9, 167.1 ppm.

General Procedure for Syntheses of Diesters

To an Ar-protected solution of 0.75 mmol of acid **1** or ***XG*** [12] in 3 cm^3 anhydrous *DMSO* was added 130 mg *CDI* (0.80 mmol), and the mixture was stirred at 45°C for 1.5 h. Then (1*S*,2*S*)- or (1*R*,2*R*)-*trans*-cyclohexanediol or diaminocyclohexane (0.25 mmol) followed by 19 mm^3 *DBU* (0.125 mmol) were added, and the mixture was stirred at 85–90°C for 16 h. After cooling, it was diluted with 150 cm^3 $CHCl_3$ and washed with 1% aq HCl (50 cm^3) and H_2O (4×100 cm^3). The solution was dried (Na_2SO_4), filtered, and after evaporation of the solvent, the residue was purified by radial chromatography and recrystallization from CH_2Cl_2–CH_3OH or ethyl acetate-hexane.

General Procedure for Syntheses of Monoesters

The syntheses of monoesters followed the same procedure as for diesters above except for the ratio acid **1** or ***XG***:cyclohexanediol was 0.50 mmol:1.00 mmol.

(+)-(1S,2S)-Cyclohexylidene bis[1-ethyl-2,7,9-trimethyl-3H,5H-dipyrrolo[1,2-c:2′,1′-f]pyrimidine-3,5-dione-8-(1,4-phenylenecarboxylate)]
(***ent*-1-*DE***, $C_{50}H_{48}N_4O_8$)

Yield 0.19 g (90%); mp 306–309°C (dec); $[\alpha]_D^{20} = +460.2\ 10^{-1} \cdot deg \cdot cm^2 \cdot g^{-1}$ ($c = 0.15$, $CHCl_3$); ^{1}H-NMR: $\delta = 1.23$ (t, $J = 7.7$ Hz, 6H), 1.52 (m, 2H), 1.65 (m, 2H), 1.86 (m, 2H), 1.97 (s, 6H), 2.05 (s, 6H), 2.28 (m, 2H), 2.56 (q, $J = 7.7$ Hz, 4H), 2.61 (s, 6H), 5.28 (m, 2H), 6.44 (s, 2H), 7.26 (m, $J = 8.4$ Hz, 4H), 8.05 (m, $J = 8.4$ Hz, 4H) ppm; ^{13}C NMR: $\delta = 8.4$, 9.7, 13.7, 13.8, 17.9, 23.5, 30.2, 74.4, 96.9, 119.6, 126.6, 126.7, 128.9, 129.0, 129.7, 129.9, 130.9, 131.8, 138.5, 143.4, 146.6, 165.8, 167.6 ppm.

(−)-(1R,2R)-Cyclohexylidene bis[1-ethyl-2,7,9-trimethyl-3H,5H-dipyrrolo[1,2-c:2′,1′-f]pyrimidine-3,5-dione-8-(1,4-phenylenecarboxylate)]
(**1-*DE***, $C_{50}H_{48}N_4O_8$)

Yield 0.17 g (81%); mp 301–308°C (dec); $[\alpha]_D^{20} = -470.0\ 10^{-1} \cdot deg \cdot cm^2 \cdot g^{-1}$ ($c = 0.23$, $CHCl_3$).

(+)-(1S,2S)-Cyclohexylidene 1-[1-ethyl-2,7,9-trimethyl-3H,5H-dipyrrolo[1,2-c:2′,1′-f]pyrimidine-3,5-dione-8-(1,4-phenylenecarboxylate)]-2-ol
(***ent*-1-*ME***, $C_{28}H_{30}N_2O_5$)

Yield 0.18 g (77%); mp 167–169°C; $[\alpha]_D^{20} = +18.9\ 10^{-1} \cdot deg \cdot cm^2 \cdot g^{-1}$ ($c = 0.42$, $CHCl_3$); ^{1}H NMR: $\delta = 1.24$ (t, $J = 7.7$ Hz, 3H), 1.42 (m, 4H), 1.77 (m, 2H), 1.98 (s, 3H), 2.10 (s, 3H), 2.17 (m, 2H), 2.57 (q, $J = 7.7$ Hz, 2H), 2.66 (s, 3H), 3.76 (m, 1H), 4.88 (m, 1H), 6.46 (s, 1H), 7.33 (m, $J = 8.4$ Hz, 2H), 8.12, (m, $J = 8.4$ Hz, 2H) ppm; ^{13}C NMR: $\delta = 8.5$, 9.7, 13.76, 13.81, 18.0, 23.7, 23.9, 30.0, 33.0, 72.8, 78.7, 96.9, 119.6, 126.68, 126.69, 129.0, 129.1, 129.7, 130.0, 130.9, 131.9, 138.7, 143.4, 146.6, 166.5, 167.7 ppm.

(−)-(1R,2R)-Cyclohexylidene 1-[1-ethyl-2,7,9-trimethyl-3H,5H-dipyrrolo[1,2-c:2′,1′-f]pyrimidine-3,5-dione-8-(1,4-phenylenecarboxylate)]-2-ol
(**1-ME**, $C_{28}H_{30}N_2O_5$)

Yield 0.16 g (69%); mp 168–170°C; $[\alpha]_D^{20} = -20.4\ 10^{-1} \cdot \text{deg} \cdot \text{cm}^2 \cdot \text{g}^{-1}$ ($c = 0.27$, $CHCl_3$).

(+)-(1S,2S)-Cyclohexylidene bis[1-ethyl-2,7,9-trimethyl-3H,5H-dipyrrolo[1,2-c:2′,1′-f]pyrimidine-3,5-dione-8-(1,2-ethylenecarboxylate)]
(***ent-XG-DE***, $C_{42}H_{48}N_4O_8$)

Yield 0.13 g (71%); mp 165–167°C; $[\alpha]_D^{20} = +129.7\ 10^{-1} \cdot \text{deg} \cdot \text{cm}^2 \cdot \text{g}^{-1}$ ($c = 0.17$, $CHCl_3$); ^{1}H NMR: $\delta = 1.19$ (t, $J = 7.7$ Hz, 6H), 1.35 (m, 2H), 1.38 (m, 2H), 1.72 (m, 2H), 1.88 (s, 6H), 1.99 (m, 2H), 2.08 (s, 6H), 2.34 (m, 4H), 2.51 (q, $J = 7.7$ Hz, 4H), 2.54 (m, 4H), 2.60 (m, 6H), 4.84 (m, 2H), 6.32 (s, 2H) ppm; ^{13}C NMR: $\delta = 8.3$, 9.0, 13.0, 13.7, 17.9, 19.2, 23.4, 30.2, 34.7, 73.8, 96.9, 120.4, 125.9, 126.0, 126.3, 130.2, 131.3, 143.1, 146.6, 167.6, 171.9 ppm.

(−)-(1R,2R)-Cyclohexylidene bis[1-ethyl-2,7,9-trimethyl-3H,5H-dipyrrolo[1,2-c:2′,1′-f]pyrimidine-3,5-dione-8-(1,2-ethylenecarboxylate)]
(***XG-DE***, $C_{42}H_{48}N_4O_8$)

Yield 0.13 g (73%); mp 164–166°C; $[\alpha]_D^{20} = -133.2\ 10^{-1} \cdot \text{deg} \cdot \text{cm}^2 \cdot \text{g}^{-1}$ ($c = 0.25$, $CHCl_3$).

(+)-(1S,2S)-Cyclohexylidene 1-[1-ethyl-2,7,9-trimethyl-3H,5H-dipyrrolo[1,2-c:2′,1′-f]pyrimidine-3,5-dione-8-(1,2-ethylenecarboxylate)]-2-ol
(***ent-XG-ME***, $C_{24}H_{30}N_2O_5$)

Yield 0.11 g (53%); mp 159–160°C; $[\alpha]_D^{20} = +24.6\ 10^{-1} \cdot \text{deg} \cdot \text{cm}^2 \cdot \text{g}^{-1}$ ($c = 0.25$, $CHCl_3$); ^{1}H NMR: $\delta = 1.21$ (t, $J = 7.7$ Hz, 3H), 1.29 (m, 4H), 1.70 (m, 2H), 1.95 (s, 3H), 2.01 (m, 2H), 2.07 (br.s, 1H), 2.13 (s, 3H), 2.47 (t, $J = 7.7$ Hz, 2H), 2.53 (q, $J = 7.7$ Hz, 2H), 2.66 (s, 3H), 2.75 (t, $J = 7.7$ Hz, 2H), 3.53 (m, 1H), 4.58 (m, 1H), 6.38 (s, 1H) ppm; ^{13}C NMR: $\delta = 8.4$, 9.2, 13.1, 13.8, 17.9, 19.4, 23.7, 23.9, 30.0, 33.1, 34.7, 72.8, 78.5, 96.9, 120.4, 125.8, 126.27, 126.30, 130.4, 131.6, 143.4, 146.5, 167.8, 172.9 ppm.

(−)-(1R,2R)-Cyclohexylidene 1-[1-ethyl-2,7,9-trimethyl-3H,5H-dipyrrolo[1,2-c:2′,1′-f]pyrimidine-3,5-dione-8-(1,2-ethylenecarboxylate)]-2-ol
(***XG-ME***, $C_{24}H_{30}N_2O_5$)

Yield 0.10 g (47%); mp 159–160°C; $[\alpha]_D^{20} = -26.9\ 10^{-1} \cdot \text{deg} \cdot \text{cm}^2 \cdot \text{g}^{-1}$ ($c = 0.30$, $CHCl_3$).

Acknowledgments

We thank the U.S. National Institutes of Health (HD-17779) for generous support of this work. Dr. *S. E. Boiadjiev* is on leave from the Institute of Organic Chemistry, Bulgarian Academy of Sciences.

References

[1] a) Kasha M, Rawls HR, El-Bayoumi MA (1965) Pure Appl Chem **11**: 371; b) McRae EG, Kasha M (1964) The Molecular Model. In: Augenstein L, Mason R, Rosenberg B (eds), International Symposium on Physical Processes in Radiation Biology. Academic Press, New York, pp 23–49

[2] Harada N, Nakanishi K (1983) Circular Dichroic Spectroscopy – Exciton Coupling in Organic Stereochemistry. University Science Books, Mill Valley, CA

[3] Berova N, Harada N, Nakanishi K (2000) Electronic Spectroscopy: Exciton Coupling, Theory and Applications. In: Lindon J, Tranter G, Holmes J (eds) Encyclopedia of Spectroscopy and Spectrometry. Academic Press, New York, pp 470–488
[4] Nakanishi K, Berova N (2000) Exciton Chirality Method – Principles and Applications. In: Nakanishi K, Berova N, Woody RW (eds) Circular Dichroism. Principles and Applications, 2nd ed. VCH, Deerfield Beach, Florida, pp 337–382
[5] Lightner DA, Gurst JE (2000) Organic Conformational Analyses and Stereochemistry from Circular Dichroism Spectroscopy. Wiley, New York, pp 423–456
[6] Hansen AaE, Bouman TD (1980) Adv Chem Phys **44**: 545
[7] Osuka A, Maruyama K (1988) J Am Chem Soc **110**: 4454
[8] Berova N, Borhan B, Dong JG, Guo J, Huang X, Karnaukhova E, Kawamura A, Lou J, Matile S, Nakanishi K, Rickman B, Su J, Tan Q, Zanze I (1998) Pure Appl Chem **70**: 377
[9] Falk H (1989) The Chemistry of Linear Oligopyrroles and Bile Pigments. Springer, Wien New York
[10] Falk H, Vormayr G, Margulies L, Mazur Y, Metz S (1986) Monatsh Chem **117**: 849
[11] a) Byun YS, Lightner DA (1991) J Org Chem **56**: 6027; b) Byun YS, Lightner DA (1991) Tetrahedron **47**: 9759
[12] Brower JO, Lightner DA (2002) J Org Chem **67**: 2713
[13] van Es JJGS, Koek JH, Erkelens C, Lugtenburg J (1986) Recl Trav Chim Pays-Bas **105**: 360
[14] Boiadjiev SE, Lightner DA (2003) J Org Chem **68**: 7591
[15] Wright SW, Hageman DL, Wright AS, McClure LD (1997) Tetrahedron Lett **38**: 7345
[16] Deziel R (1987) Tetrahedron Lett **28**: 4371; review Guibe F (1998) Tetrahedron **54**: 2967
[17] Boiadjiev SE, Lightner DA (2004) J Phys Org Chem **17**: 675
[18] Boiadjiev SE, Lightner DA (2004) J Heterocyclic Chem **41**: 1033

Verleger: Springer-Verlag GmbH, Sachsenplatz 4–6, 1201 Wien, Austria. – Herausgeber: Österreichische Akademie der Wissenschaften, Dr.-Ignaz-Seipel-Platz 2, 1010 Wien, und Gesellschaft Österreichischer Chemiker, Eschenbachgasse 9, 1010 Wien, Austria. – Redaktion: Getreidemarkt 9/163-OC, 1060 Wien, Austria. – Satz und Umbruch: Thomson Press Ltd., Chennai, India. – Offsetdruck: Manz Crossmedia, 1051 Wien, Austria. – Verlagsort: Wien. – Herstellungsort: Wien. – Printed in Austria.